

Journal of Biomedical Optics

SPIEDigitalLibrary.org/jbo

Time-lapse ultrashort pulse microscopy of infection in three-dimensional versus two-dimensional culture environments reveals enhanced extra-chromosomal virus replication compartment formation

Holly C. Gibbs
Garwin Sing
Juan Carlos González Armas
Colin J. Campbell
Peter Ghazal
Alvin T. Yeh

Time-lapse ultrashort pulse microscopy of infection in three-dimensional versus two-dimensional culture environments reveals enhanced extra-chromosomal virus replication compartment formation

Holly C. Gibbs,^a Garwin Sing,^{b*} Juan Carlos González Armas,^{c†} Colin J. Campbell,^{b,d} Peter Ghazal,^b and Alvin T. Yeh^a

^aTexas A&M University, Department of Biomedical Engineering, College Station, Texas

^bUniversity of Edinburgh, Division of Pathway Medicine, Edinburgh, United Kingdom

^cUniversity of Edinburgh, Department of Medical Microbiology, Edinburgh, United Kingdom

^dUniversity of Edinburgh, EaStCHEM, School of Chemistry, Edinburgh, United Kingdom

Abstract. The mechanisms that enable viruses to harness cellular machinery for their own survival are primarily studied in cell lines cultured in two-dimensional (2-D) environments. However, there are increasing reports of biological differences between cells cultured in 2-D versus three-dimensional (3-D) environments. Here we report differences in host-virus interactions based on differences in culture environment. Using ultrashort pulse microscopy (UPM), a form of two-photon microscopy that utilizes sub-10-fs pulses to efficiently excite fluorophores, we have shown that *de novo* development of extra-chromosomal virus replication compartments (VRCs) upon murine cytomegalovirus (mCMV) infection is markedly enhanced when host cells are cultured in 3-D collagen gels versus 2-D monolayers. In addition, time-lapse imaging revealed that mCMV-induced VRCs have the capacity to grow by coalescence. This work supports the future potential of 3-D culture as a useful bridge between traditional monolayer cultures and animal models to study host-virus interactions in a more physiologically relevant environment for the development of effective anti-viral therapeutics. These advances will require broader adoption of modalities, such as UPM, to image deep within scattering tissues. © The Authors. Published by SPIE under a Creative Commons Attribution 3.0 Unported License. Distribution or reproduction of this work in whole or in part requires full attribution of the original publication, including its DOI. [DOI: [10.1117/1.JBO.18.3.031111](https://doi.org/10.1117/1.JBO.18.3.031111)]

Keywords: murine cytomegalovirus; replication compartment; time-lapse two-photon microscopy.

Paper 12655SSR received Oct. 1, 2012; revised manuscript received Dec. 28, 2012; accepted for publication Jan. 18, 2013; published online Mar. 1, 2013.

1 Introduction

Viruses have evolved complex molecular mechanisms to interact with their host genomes and utilize cellular machinery to ensure their reproduction and survival. These molecular mechanisms, which are useful targets for anti-viral drugs, have traditionally been studied in two-dimensional (2-D) cell cultures. However, many groups are reconsidering use of 2-D culture environments (i.e., tissue culture flasks, Petri dishes, and well plates) as increasing evidence suggests that cellular properties such as cytoskeletal arrangement, signal transduction, and cell differentiation, differ when cells are grown as 2-D monolayers compared to in a three-dimensional (3-D) environment.¹⁻³ These findings make intuitive sense, because a 3-D environment, including an extracellular matrix, more closely mimics a cell's natural chemical and mechanical tissue micro-environment in the body.^{4,5}

Differences in host-virus interaction dependent on culture environment have been previously reported,^{6,7} including culture-dependent hepatitis C virus (HCV) host-virus biology.^{8,9} HCV is a leading cause of chronic hepatitis worldwide, but patient-

derived HCV strains cannot be effectively propagated in traditional monolayer cultures.¹⁰ So HCV infection could be studied *in vitro*, a recombinant HCV strain was developed that propagates in immortalized hepatocytes grown as monolayers.¹¹ This recombinant culture system is limited in its relevance, however, motivating investigations utilizing different culture conditions, including hepatocytes cultured in a 3-D gel matrix that have been shown to better support the replication of clinical HCV isolates.^{12,13} This example illustrates that in order to better characterize host-virus interactions and improve virus culture, it may be worth the added complexity of 3-D culture systems to maintain a more physiologically relevant microenvironment.¹⁰ This shift to 3-D cultures introduces the challenge of imaging deeper in a more highly scattering environment.

In this study, we have used two-photon (2P) microscopy utilizing ultrashort, sub-10-fs pulses, which we call ultrashort pulse microscopy (UPM), to investigate differences in host-virus biology due to culture environment using cytomegalovirus (CMV) as a model for infection. Human cytomegalovirus (HCMV) is a ubiquitous virus that poses a serious problem for immune-compromised patients and neonates with immature immune systems, resulting in congenital malformations.^{14,15} mCMV, a murine homolog of HCMV, is an established model to study various aspects of CMV pathology both in animals (*in vivo*) and in culture (*in vitro*). Immortalized NIH 3T3 mouse fibroblasts are permissive to mCMV infection, and we selected this model since its cellular pathology is robust and well

*Present address: Alfaisal University, Riyadh, Saudi Arabia.

†Present address: Instituto de Investigación Hospital 12 de Octubre, Madrid, Spain.

Address all correspondence to: Holly C. Gibbs, Texas A&M University, Department of Biomedical Engineering, College Station, Texas. Tel: 1 979 845 8811; Fax: 1 979 845 4450; E-mail: holly.gibbs.bme@gmail.com

characterized. Sub-10-fs pulses utilized in UPM have very high peak powers (MJ), however, the overall average power deposited in cells is lower than in conventional 2P systems. The broadband spectrum of sub-10-fs pulses also leads to a large 2P power spectrum that efficiently excites fluorescence from a broad range of intrinsic and extrinsic fluorophores simultaneously.^{16,17} Consequently, UPM generates high 2P signals while preserving sample integrity and is thus ideal for time-lapse imaging.

2 Materials and Methods

2.1 Generation of NIH-3T3/H2B-GFP Cell Line and FACS Analysis

NIH-3T3 cells were transfected with 2 mg of H2B-GFP expression vector¹⁸ using LipofectAMINE according to manufacturer's protocol (Gibco BRL, San Francisco, CA). Two days after transfection, medium was changed and 10 mg/ml blasticidine-S (EMD Millipore, Billerica, MA) was added. Five days later, the medium was changed to 2 mg/ml blasticidine-S. After 15 days of drug selection, cells were collected and cloned by limiting dilution with selection. Several clones were expanded and cultured for three months in the absence of blasticidine-S. Five of these clones continued strong GFP-H2B expression, which suggests that chromosome stability is unimpaired by constitutive H2B-GFP expression, and were selected for fluorescence activated cell sorting (FACS) analysis.

For FACS analysis, NIH-3T3 cells expressing the H2B-GFP construct were harvested by trypsinization and fixed in 70% ethanol for more than 3 h at 4°C. Cells were stained with PI (20 mg/ml) containing RNase (200 ng/ml). Fluorescence was measured using a FACScan (Becton Dickinson, Mountain view, CA). The red (PI) and green (GFP) emissions from each cell were used to measure DNA content and GFP-H2B fluorescence, respectively. Cell debris and fixation artifacts were gated out using Cell Quest software (Becton Dickinson). The brightest clone with normal cell cycle distribution, clone #2, was selected for further use.

2.2 Cell and Virus Cultures

NIH-3T3/H2B-GFP cells were maintained at 37°C in a 5% CO₂ atmosphere in Dulbecco's modified Eagle's medium (DMEM) supplemented with 10% calf serum (CS), 2 mM L-glutamine, 100 U/ml penicillin and 100 mg/ml streptomycin. The Smith strain of mCMV (a gift from Dr. Ann Campbell, Eastern Virginia Medical School) was used, and stocks prepared in NIH-3T3 cells. Viral titers were determined by standard plaque assays.

For analyzing viral replication compartment (VRC) formation, NIH-3T3/H2B-GFP cells grown in 12-well dishes at 70% confluence were infected with mCMV at a multiplicity of infection (MOI) of 10 plaque forming units per cell (PFU/cell) with inoculum prepared with DMEM and 2% CS. After 1 h adsorption period at 37°C, the inoculum was removed, the cell cultures were washed once with phosphate-buffered saline (PBS), and fresh DMEM with 10% CS was added. For 3-D cultures, collagen gels were assembled with rat-tail type I collagen (Becton Dickinson), 5X DMEM, and reconstitution buffer, and neutralized with 1 M NaOH. NIH-3T3 cells were seeded in gels at 70% density (v/v) and were subsequently allowed to polymerize and equilibrate at 37°C and 5% CO₂ in

12-well plates. Gels were infected with mCMV approximately one day later, also at a MOI of 10 under the same conditions as cells grown as monolayers in 12-well dishes.

2.3 Ultrashort Pulse Microscopy

The custom-built laser-scanning two-photon microscope used for ultrashort pulse microscopy (UPM) has been previously described.¹⁹ Briefly, sub-10-fs pulses from a passively mode-locked Ti:Sapphire oscillator with 800 nm center wavelength and 133 nm full-width half maximum (Femtolasers, Vienna, Austria) were pre-compensated (GSM 270, Femtolasers) and coupled by a galvanometer driven X-Y scanner (Cambridge Technology, Cambridge MA) into an upright microscope (Axioskop2 MAT, Carl Zeiss). The beam was directed by a 635 nm short pass dichroic mirror (Chroma, Bellows Falls, VT) through the imaging objective to the sample. The two-photon excited GFP signal was then collected through the imaging objective (63X, 1.2 NA and 40X, 0.8 NA from Carl Zeiss) and separated using a 430 nm long-pass dichroic mirror (Chroma), further discriminated with a 525/50 nm bandpass filter (Chroma), and detected with a PMT (Hamamatsu, Bridgewater, NJ). Data acquisition was controlled with custom LabVIEW software (National Instruments, Austin, TX).

For time-lapse imaging, cell cultures were imaged in custom-built environmental chamber and maintained at 35°C with 5% CO₂ with 3-5 mW power at the sample. Z-stacks were acquired every fifteen minutes at 0.5 μm steps over the course of imaging.

2.4 Image Processing

Z-stacks were converted to raw intensity images of chromatin structure (from GFP-H2B) with custom Matlab software (Mathworks, Natick, MA) and subsequent processing and quantification were performed with custom semi-automated Matlab routines. Three-dimensional reconstructions and VRC tracking were performed with ImageJ open source software.

To quantify chromosomal volume, we segmented the GFP-H2B signal. Each optical section from a z-stack was converted to binary mask with an automated algorithm based on Otsu's method that minimizes intraclass variance between background (noise) and foreground (GFP-H2B) pixels. The sum of all binary masks in a z-stack was then converted from total number of voxels to spatial volume using the measured dimensions of each voxel for 63X and 40X objectives.

To quantify nuclear volume, we outlined the GFP-H2B signal and filled in that region to generate a mask of total nuclear area for each optical section. A binary mask was generated from each optical section of a z-stack with a 50% lower threshold than above, which better preserved the outline of the nucleus from the chromatin structure. To join edges that remained discontinuous in the outline of the nucleus, the binary mask was dilated using a 5 pixel structural disc-shaped element. The mask was then eroded using the same structural element to recover the original boundary with continuous edges and remaining negative spaces within the nucleus converted to 1's. As with chromosomal volume, the sum of all binary masks in a z-stack was then converted from total number of voxels to spatial volume using the measured dimensions of each voxel for 63X and 40X objectives.

3 Results

By transfection of NIH-3T3 cells with the H2B-GFP mammalian expression vector¹⁸ and selection with blasticidin, we

obtained a polyclonal cell population that stably expressed an H2B-GFP transgene for tracking chromatin dynamics. Isolated clones were selected by FACS and by comparison of cell cycle distribution to those of the parental line [Fig. 1(a)]. Using UPM, we imaged these NIH 3T3/H2B-GFP cells infected with mCMV either as adherent monolayers in tissue culture plates or in collagen gels. In both 2-D and 3-D environments, cells were cultured in DMEM with 10% CS and inoculated in DMEM with 2% CS with the same number of plaque forming units (PFU) of virus per cell so that MOI was kept constant at 10 PFU/cell. The collagen gel (3 mg/ml) used to construct

the 3-D culture was seeded so that the cell density at the time of inoculation was 70% (volume), and in 2-D, cells were inoculated at 70% confluence (area). 2P signal generated from the GFP-H2B fusion was used to quantify nuclear parameters, similar to what has been previously reported [Fig. 1(c)].²⁰ Briefly, semiautomated algorithms in Matlab were used to threshold the GFP signal to binary masks that were summed to find a cell's chromatin volume. Then morphological operations (fill, dilate, and erode) were used on each 2-D mask to generate a smooth mask of the nucleus that was summed in 3-D for calculating total nuclear volume. The difference

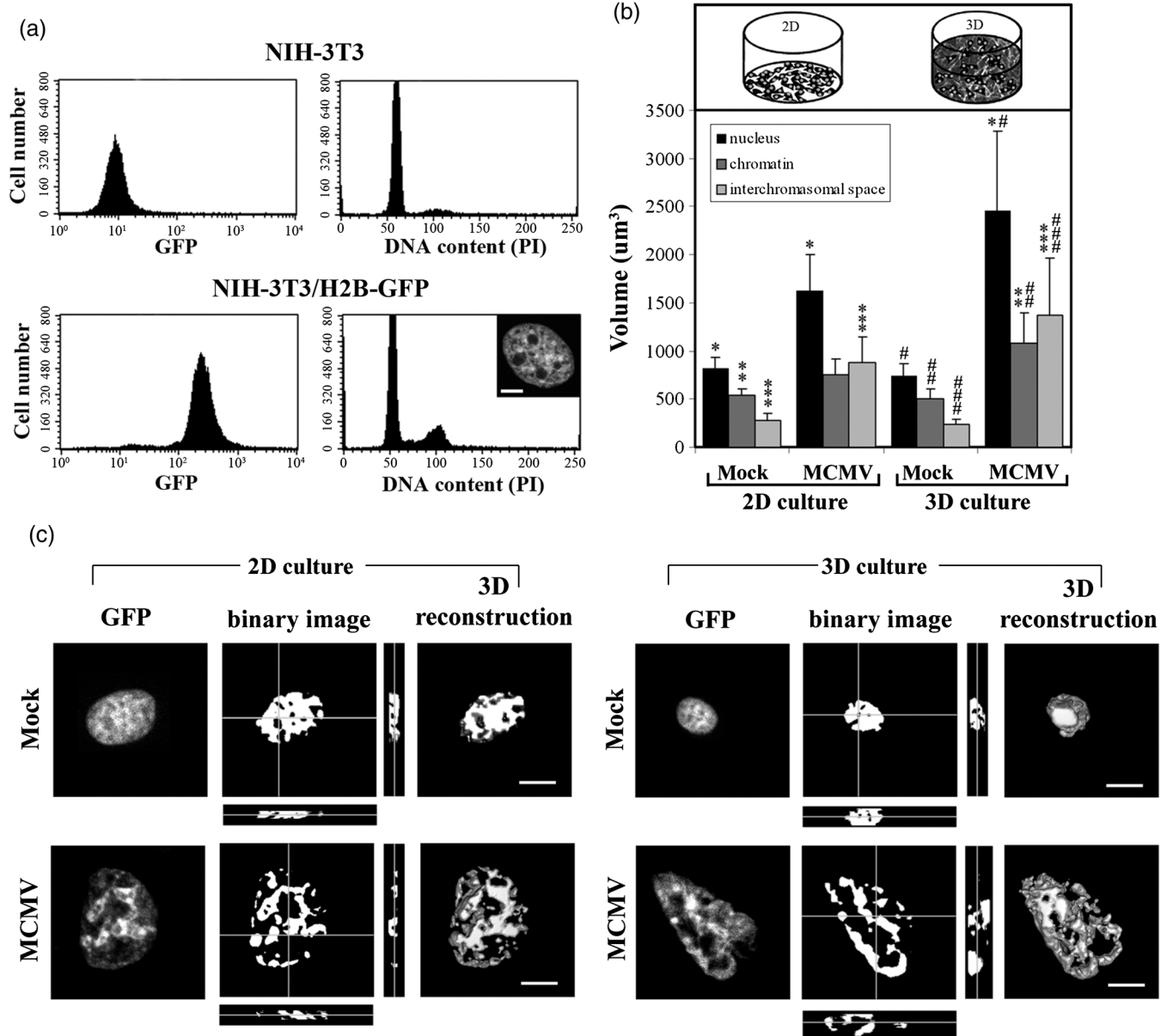


Fig. 1 Quantification of chromatin and nuclear volume during viral replication compartment (VRC) formation in mCMV infected NIH-3T3/H2B-GFP cells grown on 2-D or 3-D substrates. (a) Flow cytometry was used to isolate NIH-3T3/H2B-GFP clones. (b) NIH-3T3/H2B-GFP cells were grown either on a plastic surface or seeded in a collagen type I gel (top). UPM and image segmentation reveal that mCMV infection results in a significant increase in nuclear volume coupled with the expansion of VRCs for NIH-3T3/H2B-GFP cells grown on 2-D plastic surface at 8 hours post infection (hpi) (matched asterisk and pound symbols denote significant differences, $p < 0.01$). Similar behavior was observed in NIH-3T3/H2B-GFP cells infected at the same multiplicity of infection grown in collagen gels, however, the expansion of the nucleus due to increases in interchromosomal volume and chromatin volume was significantly larger ($p < 0.01$). No significant difference in chromatin or nuclear volume was measured between mock-infected 2-D and 3-D cultures. (c) Optical sectioning with ultrashort pulse microscopy shows host chromatin structure is disrupted by large VRCs in mCMV infected NIH-3T3/H2B-GFP cells compared to mock-infected cells at 8 hpi (scale bar = 5 μm , lines indicate section planes).

between the total nuclear volume and chromosomal volume is what we refer to as the interchromosomal volume. The z-axis was oversampled (step size = 0.5 μm) so no chromosome details would be lost. 3-D reconstructions and VRC tracking were performed with ImageJ.

First, we imaged the cultures at 8 hours post infection (hpi), when the virus is known to be actively replicating.²¹ We found that at 8 hpi, the nuclear volume increases significantly due to expansion of VRCs (measured indirectly by expansion of interchromosomal space) in both 2-D and 3-D culture environments compared to mock infected controls. Interestingly, however, the increase in nuclear volume for infected NIH 3T3s cultured in collagen gels was significantly larger than the increase for infected NIH 3T3s cultured on well plates [Fig. 1(b)]. No compression of the host chromatin was measured at this point in the infection. Importantly, these data indicate that the extracellular matrix does not impede efficient infection of NIH 3T3s by mCMV and subsequent viral replication. In fact, the 3-D collagen culture environment enhances these processes either directly or indirectly.

We also characterized the dynamics of VRC formation from 8 to 16 hpi using UPM. Mock-infected cells maintain constant nuclear and chromatin volume between 8 and 16 hpi [Fig. 2(a) and 2(b)]. In both 2-D and 3-D culture environments, the nature

of mCMV infection changed during the course of imaging, shifting from an expansion of nuclear volume with unchanged chromatin volume from 8 to 12 hpi to a dramatic decrease in both nuclear and chromatin volume from 12 to 16 hpi [Fig. 2(a) and 2(b)], indicating a compression phase. These findings are similar to those previously reported for the related alpha-herpes virus HSV-1.²⁰ We observed a trend of somewhat slower rate of decrease in nuclear and chromatin volume in 3-D culture compared to 2-D culture, but this was statistically insignificant. We also observed a characteristic cytopathic effect of lytic infection begin to appear in both 2-D and 3-D cultures at approximately 16 hpi [arrows, Fig 2(a) and 2(b)]. This pathological feature, marked by the buckling of the nucleus, is more dramatic in the 3-D culture environment. Also of note, chromatin structure of the controls was remarkably stable over time, highlighting the usefulness of UPM for extended periods of live-cell imaging in both 2-D and 3-D culture environments.

Finally, utilizing the sub-cellular resolution of UPM, we tracked the dynamics of individual replication compartments within NIH 3T3 cells infected with mCMV in 3-D collagen cultures from 8 to 24 hpi [Fig. 3(a) and Video 1]. Our goal was to see if individual VRCs coalesce to form larger VRCs, as has been previously reported for the related alpha-herpes virus

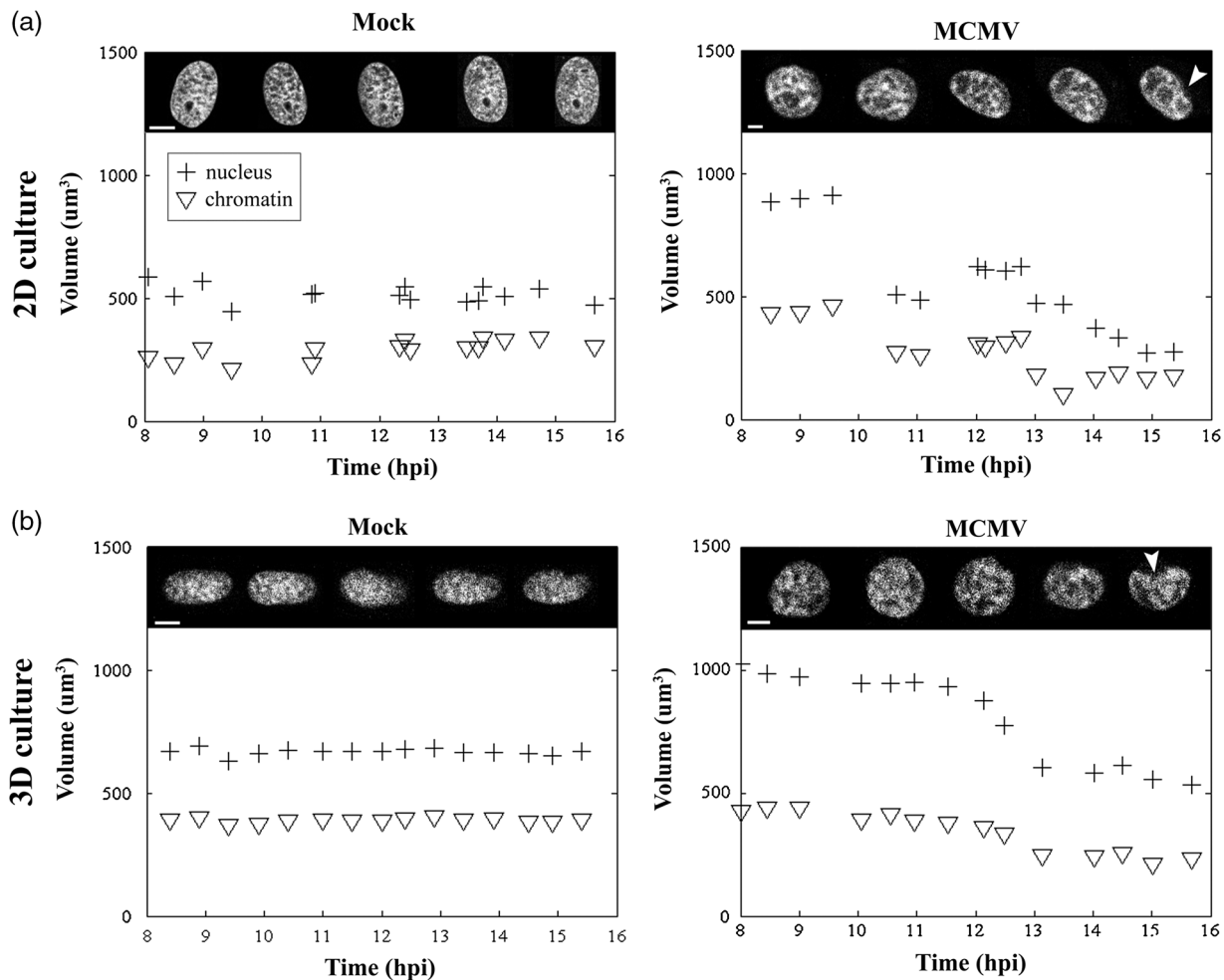


Fig. 2 Evolution of VRCs in mCMV infected NIH-3T3/H2B-GFP cells grown in 2-D or 3-D cultures. Representative plots of nucleus (cross) and chromatin (triangle) volume derived from time-lapse UPM from 8 to 16 hpi show dynamic compression of NIH-3T3/H2B-GFP chromatin and decrease in nuclear volume at late stages of mCMV infection in 2-D (a) and 3-D (b) cultures ($n = 4$, scale bar = 5 μm). Arrowheads point to the buckling morphology of the infected nuclei by 16 hpi, which is more dramatic at that time in 3-D cultures.

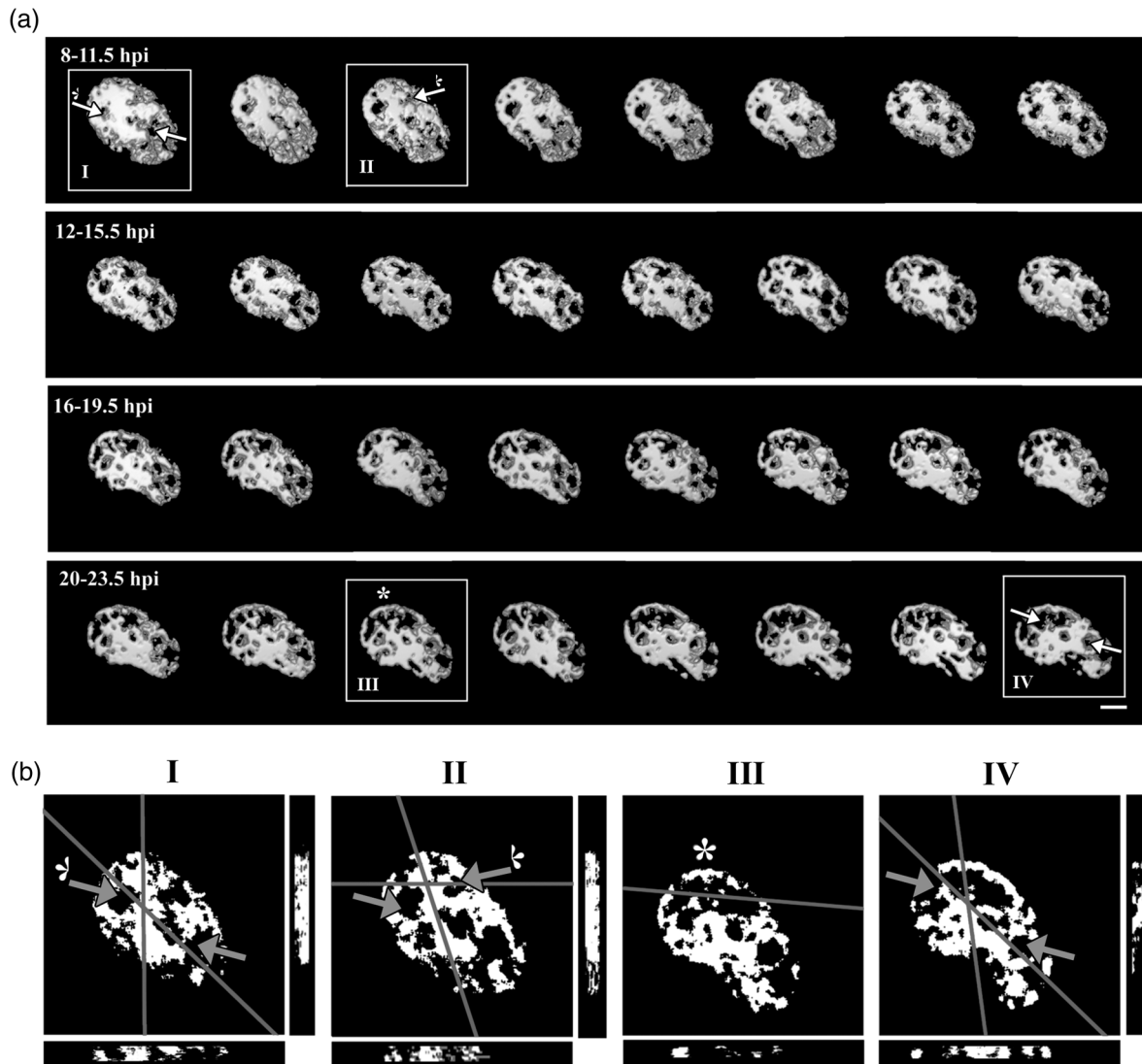


Fig. 3 Dynamic tracking of mCMV VRCs in NIH-3T3/H2B-GFP cells in 3-D culture. (a) 3-D reconstructions of optical sections obtained from time-lapse UPM of mCMV-infected NIH-3T3/H2B-GFP cells seeded in collagen gels from 8 to 24 hpi show smaller VRCs fuse together to form larger compartments. Arrows indicate initial VRCs while asterisks follow the VRCs that will fuse and the observed fusion event (scale bar = 5 μ m) (b) Examination of individual sections (lines indicate section planes) reveals that the VRCs initially identified (I) can fuse with independent VRCs (II, III) but remain distinct from each other up to 24 hpi (IV). (Video 1, MOV, 14.5 MB) [URL: <http://dx.doi.org/10.1117/1.JBO.18.3.031111.1>].

HSV-1.²² In this study, two easily distinguishable VRCs were identified at 8 hpi, marked by arrows [Fig 3(bI)]. Sections from the lines on the image illustrate the separation of these VRCs by host chromatin and that they are indeed distinct from each other. Another separate VRC was identified at 9 hpi and marked also with an arrow [Fig. 3(bII)]. The two VRCs with arrows marked with an asterisk coalesce at 20 hpi [Fig. 3(bIII)], but by 24 hpi, the two originally identified VRCs remain distinct. These data demonstrate similarities in the mechanisms of replication compartment formation and marginalization of host chromatin between alpha-herpesvirus HSV-1 and beta-herpesvirus mCMV.

4 Discussion

Using UPM, we have demonstrated differences in host-virus interactions dependent on culture environment using mCMV as a model. Based on our studies, we conclude that the 3-D culture environment promotes expansion and prolongation of

inter-chromosomal VRCs upon mCMV infection. Although the density of the extracellular matrix would be expected to impede the attachment of virus particles to the host cell, we found that this was not the case, in fact virus infection and replication was enhanced when 3T3 fibroblasts were cultured in a collagen matrix. While other studies of virus infection of cells in a 3-D collagen gels are rare, there is some precedent. Using a GFP labeled Sindbis virus, it was shown that virions penetrated the collagen matrix to infect baby hamster kidney cells.²³ Our work supports their study, as we have clearly seen pathological phenotypes of mCMV infected NIH 3T3 fibroblasts cultured in collagen gels.

The immortalized NIH 3T3 cellular phenotype may change significantly in 3-D culture in response to mechano-chemical cues, contributing to the differences we see in this study. Relevant to the differences previously reported in HCV, differentiation of human embryonic stem cells into hepatocytes has been shown under 3-D fluid culture conditions.²⁴ In fact, by 3-D culture, immortalized hepatocytes that have been cultured

in a 2-D environment for long periods of time can be induced to switch to a phenotype that more closely matches liver tissue.¹⁰ This switch highlights the plasticity of cells and their sensitivity to their microenvironments. It would be interesting to profile the gene expression of NIH 3T3 fibroblasts in 2-D versus 3-D environments to identify candidate host proteins that may interact with virus proteins to account for the differential productivity of infection of 3T3s by mCMV in these contrasting environments.

Using 3-D culture and time-lapse UPM, we have also drawn important conclusions about the relatedness of alpha- and beta-herpes viruses by showing that, similar to what has been reported before for HSV-1, mCMV replication compartments follow the expansion-marginalization model²⁰ and coalesce to form larger replication compartments.

Our study points toward the growing need to study environmental factors resulting in culture dependent host-virus biology. We did not explore how mechanical properties of the ECM may affect host-virus interaction, though recently it has been shown that some cells are more or less sensitive to TGF- β induced apoptosis depending on extracellular matrix stiffness when chemical composition is kept constant.²⁵ In the future, with combined nonlinear optical microscopy and optical coherence microscopy²⁶ which can optically differentiate extracellular matrix components such as collagen, fibrin, and elastin,^{27,28} we can examine in more detail this intersection of mechano-transduction and immune signaling.^{29,30}

Acknowledgments

We would like to acknowledge the Texas-UK Collaborative Initiative, National Science Foundation, and Wellcome Trust for supporting this work.

References

1. F. Wang et al., "Reciprocal interactions between beta 1-integrin and epidermal growth factor receptor in three-dimensional basement membrane breast cultures: A different perspective in epithelial biology," *Proc. Natl. Acad. Sci. U. S. A.* **95**(25), 14821–14826 (1998).
2. M. Schindler et al., "Living in three dimensions—3D nanostructured environments for cell culture and regenerative medicine," *Cell Biochem. Biophys.* **45**(2), 215–227 (2006).
3. A. Birgersdotter, R. Sandberg, and I. Ernberg, "Gene expression perturbation *in vitro*—a growing case for three-dimensional (3D) culture systems," *Sem. Cancer Biol.* **15**(5), 405–412 (2005).
4. G. Andrei, "Three-dimensional culture models for human viral diseases and antiviral drug development," *Antiviral Res.* **71**(2–3), 96–107 (2006).
5. Y. T. Wang et al., "Dendritic cells treated with HPV16mE7 in a three-dimensional model promote the secretion of IL-12p70 and IFN-gamma," *Exp. Mol. Pathol.* **91**(1), 325–330 (2011).
6. C. Johnson and H. Fan, "Three-dimensional culture of an ovine pulmonary adenocarcinoma-derived cell line results in re-expression of surfactant proteins and Jaagsiekte sheep retrovirus," *Virology* **414**(1), 91–96 (2011).
7. Y. Tanaka et al., "Development of novel three-dimensional longterm culture system of human hepatocytes for hepatitis B virus infection," *Hepatology* **44**(4), 541A–541A (2006).
8. "National Institutes of Health Consensus Development Conference Statement: management of hepatitis C: 2002—June 10-12, 2002," *Hepatology* **36**(5), S3–S2 (2002).
9. K. Moriya et al., "The core protein of hepatitis C virus induces hepatocellular carcinoma in transgenic mice," *Nat. Med.* **4**(9), 1065–1067 (1998).
10. H. H. Aly, K. Shimotohno, and M. Hijikata, "3D cultured immortalized human hepatocytes useful to develop drugs for blood-borne HCV," *Biochem. Biophys. Res. Commun.* **379**(2), 330–334 (2009).
11. K. J. Blight, A. A. Kolykhalov, and C. M. Rice, "Efficient initiation of HCV RNA replication in cell culture," *Science* **290**(5498), 1972–1974 (2000).
12. K. Murakami et al., "Production of infectious hepatitis C virus particles in three-dimensional cultures of the cell line carrying the genome-length dicistronic viral RNA of genotype 1b," *Virology* **351**(2), 381–392 (2006).
13. B. Sainz, V. TenCate, and S. L. Uprichard, "Three-dimensional Huh7 cell culture system for the study of hepatitis C virus infection," *Virol. J.* **6**, 103 (2009).
14. T. Crough and R. Khanna, "Immunobiology of human cytomegalovirus: from bench to bedside," *Clin. Microbiol. Rev.* **22**(1), 76–98 (2009).
15. C. H. Cook and J. Trgovcich, "Cytomegalovirus reactivation in critically ill immunocompetent hosts: a decade of progress and remaining challenges," *Antiviral Res.* **90**(3), 151–159 (2011).
16. S. Pang et al., "Beyond the 1/T-p limit: two-photon-excited fluorescence using pulses as short as sub-10-fs," *J. Biomed. Opt.* **14**(5), 054041 (2009).
17. C. Wang and A. T. Yeh, "Two-photon excited fluorescence enhancement with broadband versus tunable femtosecond laser pulse excitation," *J. Biomed. Opt.* **17**(2), 025003 (2012).
18. T. Kanda, K. F. Sullivan, and G. M. Wahl, "Histone-GFP fusion protein enables sensitive analysis of chromosome dynamics in living mammalian cells," *Curr. Biol.* **8**(7), 377–385 (1998).
19. A. M. Larson and A. T. Yeh, "Ex vivo characterization of sub-10-fs pulses," *Opt. Lett.* **31**(11), 1681–1683 (2006).
20. K. Monier et al., "Annexation of the interchromosomal space during viral infection," *Nat. Cell Biol.* **2**(9), 661–665 (2000).
21. A. Angulo et al., "Enhancer requirement for murine cytomegalovirus growth and genetic complementation by the human cytomegalovirus enhancer," *J. Virol.* **72**(11), 8502–8509 (1998).
22. T. J. Taylor et al., "Herpes simplex virus replication compartments can form by coalescence of smaller compartments," *Virology* **309**(2), 232–247 (2003).
23. D. C. Thach and D. A. Stenger, "Effects of collagen matrix on Sindbis virus infection of BHK cells," *J. Virol. Methods* **109**(2), 153–160 (2003).
24. T. Miki, A. Ring, and J. Gerlach, "Hepatic differentiation of human embryonic stem cells is promoted by three-dimensional dynamic perfusion culture conditions," *Tissue Eng. Part C-Methods* **17**(5), 557–568 (2011).
25. P. Godoy et al., "Extracellular matrix modulates sensitivity of hepatocytes to fibroblastoid dedifferentiation and transforming growth factor beta-induced apoptosis," *Hepatology* **49**(6), 2031–2043 (2009).
26. Q. F. Wu, B. E. Applegate, and A. T. Yeh, "Cornea microstructure and mechanical responses measured with nonlinear optical and optical coherence microscopy using sub-10-fs pulses," *Biomed. Opt. Express* **2**(5), 1135–1146 (2011).
27. L. E. Niklason et al., "Enabling tools for engineering collagenous tissues integrating bioreactors, intravital imaging, and biomechanical modeling," *Proc. Natl. Acad. Sci. U. S. A.* **107**(8), 3335–3339 (2010).
28. Y. Bai et al., "Intravital characterization of engineered tissues by multimodal optical imaging and biaxial mechanical testing," (in submission).
29. K. Valyi-Nagy et al., "Identification of virus resistant tumor cell subpopulations in three-dimensional uveal melanoma cultures," *Cancer Gene Therap.* **17**(4), 223–234 (2010).
30. A. Birgersdotter et al., "Three-dimensional culturing of the Hodgkin lymphoma cell-line L1236 induces a HL tissue-like gene expression pattern," *Leukemia Lymphoma* **48**(10), 2042–2053 (2007).